

Determination of residual stress in Cr-implanted Al₂O₃ by glancing angle x-ray diffraction

E. D. Specht, C. J. Sparks, and C. J. McHargue

Metals and Ceramics Division, Oak Ridge National Laboratory, Oak Ridge, Tennessee 37831-6118

(Received 9 December 1991; accepted for publication 24 February 1992)

We report x-ray diffraction measurements of residual stress in sapphire crystals implanted with Cr⁺ ions. Stress is determined by measuring both in-plane and out-of-plane lattice constants. Bragg peak positions are measured to determine average stress, while peak widths are measured to determine its variation. Using angles of incidence close to the critical angle for total external reflection of x rays, we compare measurements confined to within ~2.5 nm of the surface and measurements over the ~80 nm thickness of the implanted region. These x-ray residual stress determinations are consistent with those based on indentation crack length, but were less by a factor of 10 than reports based on cantilever bending.

Brittle materials such as ceramics are much stronger in compression than in tension. Methods for exploiting this high strength include a variety of techniques for prestressing so that the material remains in compression for both compressive and tensile added loads.¹ Because a thin plate becomes unstable under a large compressive in-plane stress, it is particularly useful for such a geometry to prestress the surface only—provided that cracks do not nucleate inside the sample. Kirchner² reviews the strengthening of ceramics by compressive surface stresses produced by thermal quenching, chemical treatment, and phase transformation.

Ion implantation is a more recently developed means of producing a compressive surface stress, which can result from defect production, phase transformation, amorphization, or change in chemical composition. White *et al.*³ reviewed the effect of ion implantation on ceramics. Increases of up to 65% have been reported in the flexure strength of ion-implanted sapphire.⁴⁻⁷ While compressive surface stresses have been observed in strengthened samples using cantilever bending⁵ and indentation fracture^{6,7} techniques, the magnitude of the stress remains uncertain. In the only direct comparison of the two techniques, a bending measurement indicated stresses a factor of 10 higher than indentation.⁸ Comparison of bending and indentation stress measurements of samples prepared under different conditions appears to support this trend.³

In this letter, we report x-ray diffraction measurements of the surface stress in Cr⁺-implanted Al₂O₃ single crystals, describing techniques we have developed to measure the strain in a thin layer on a weakly absorbing substrate. Because Al₂O₃ and Cr₂O₃ are completely soluble,⁹ no other crystalline phases form, making this a simple model system. X-ray diffraction has often been used to measure the effects of ion implantation.¹⁰⁻¹⁸ Because these earlier studies analyzed samples for which the x-ray penetration depth is comparable to the ion penetration depth, standard techniques were applied in which x rays are incident at a large angle of incidence. In contrast, the fracture resistance of sapphire is increased by implantation to a depth of just 10⁻³ of the x-ray penetration depth in sapphire (79 μm at 8.04 keV), so diffraction at a large angle of incidence pro-

vides insufficient sensitivity to the implanted region. As demonstrated by Wallner *et al.*,¹⁹ the use of smaller incident angles provides sensitivity to a thin implanted layer. By using angles of incidence close to the critical angle for total external reflection of x rays, we vary the penetration depth between 2.5 nm and 1 μm and present stress measurements for both the uppermost part of and the whole of the implanted region. In addition to measurement of out-of-plane strain, as in Refs. 10-18, we include measurements of the in-plane strain of the implanted region to test the assumption that the strained layer is constrained in-plane by the substrate.

High-purity Al₂O₃ crystals with nominal [00.1] surface normals were given an optical grade polish and annealed for 120 h at 1500 °C in flowing oxygen to remove residual polishing damage. They were implanted at room temperature using a mass analyzed 160 keV ion beam of ⁵²Cr⁺ in a Varian 200 kV implanter. The ion beam was directed 7° off normal to minimize channeling effects. According to calculations using E-DEP code,²⁰ the ions have a range of 79 ± 26 nm; energy is lost with fair uniformity up to this depth. Thus, the 50 nm nearest the surface will be heavily damaged but free of Cr. A deeper x-ray penetration depth will include the implanted region. Samples implanted with 1 × 10¹⁷ and 4 × 10¹⁶ Cr⁺/cm² were studied, along with an unimplanted control.

X-ray diffraction measurements were made with a Cu target rotating anode source operating at 8 kW. The sample was mounted on a four-circle diffractometer. A Ge(111) incident beam monochromator and slits selected the CuKα₁ wavelength and defined a 1 × 1 mm² incident beam with 2.8 × 10⁵ photons/s and a divergence of 0.010° in-plane (horizontal) × 0.053° out-of-plane (vertical). The narrow out-of-plane divergence is needed to control the incident glancing angle. The surface normal direction was located to within 0.02° by measuring the angle of specular reflection. Because the surface normal deviated from the [00.1] direction by between 1.2° and 2.0° for each sample, we were able to measure (*h*, *k*, 0) Bragg peaks at positive glancing angles. Scans were taken at constant incident glancing angle α as described by Mochrie.²¹

For the measurement of in-plane peaks, a Ge(111)

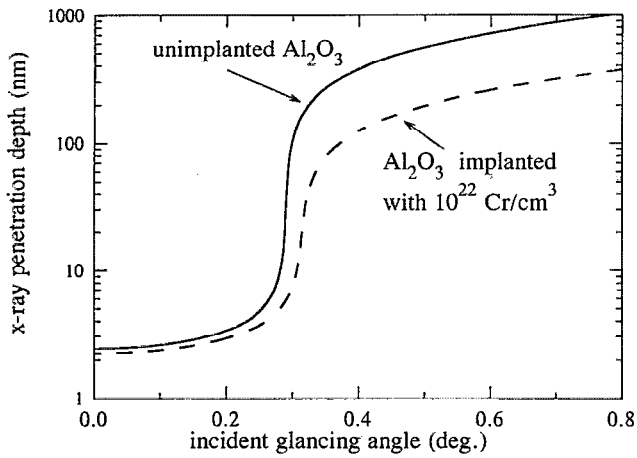


FIG. 1. X-ray penetration depth from Eq. (1) for pure Al_2O_3 and with the effect of implanted Cr.

analyzing crystal was used to provide narrow in-plane and wide out-of-plane resolution. Scans about each $(h, k, \cdot, 0)$ peak were taken in a two-dimensional grid covering the radial $[h, k, \cdot, 0]$ and transverse $[-h-2k, 2h+k, \cdot, 0]$ directions. For out-of-plane peaks, slits were used to define the diffracted beam direction. Slits were set to exclude scattering from the crystal edges and to provide narrow resolution (0.10°) in the out-of-plane direction and wide resolution (0.50°) in the in-plane direction. Scans were taken through Bragg peaks in the $[00.1]$ direction.

The effect of small incident glancing angle α on diffraction has been described by Vineyard.²² While the component of the wave vector parallel to the surface is unaffected by refraction, the normal component changes from $k_z = -(2\pi/\lambda)\sin\alpha$ to

$$k'_z = -\frac{2\pi}{\lambda} \left(\sin^2\alpha - \sin^2\alpha_c + \frac{i\mu\lambda}{2\pi} \right)^{1/2}. \quad (1)$$

The critical angle α_c is given by $\sin^2\alpha_c = \rho e^2 \lambda^2 / (\pi m c^2)$. μ is the linear x-ray absorption coefficient, λ the wavelength, ρ the electron density, e and m the electron charge and mass, and c the speed of light. For pure Al_2O_3 , and $\text{CuK}\alpha_1$ x rays, $\alpha_c = 0.29^\circ$ and $\mu = 0.0127 \mu\text{m}^{-1}$. This has two effects: reciprocal lattice points are shifted by $\text{Re}(k'_z - k_z)$, and the x-ray penetration depth is reduced to $|2 \text{Im}(k'_z)|^{-1}$. Figure 1 shows the penetration depth as a function of incident glancing angle. We include a calculation for Al_2O_3 implanted with $1 \times 10^{22} \text{ Cr/cm}^3$ (assuming no lattice expansion), as well as for pure Al_2O_3 , to give an estimate of the effect from changes in composition.

For measurements of the in-plane lattice constant there is neither a shift due to refraction nor any instrumental broadening due to the finite penetration depth; for the unimplanted control, the full width at half-maximum (FWHM) of the (30.0) rocking curve remains the instrumental width of 0.04° as α is varied from 0.8° to 0.1° . Measurements at $\alpha = 0.25^\circ$ of radial and transverse widths of the (11.0), (30.0), and (22.0) peaks of the 10^{17} sample reveal a broadening due to strain, with $\Delta a/a = 0.0015$ FWHM. For the 4×10^{16} sample, broadening of the (30.0) peak indicates an in-plane strain of 0.00057. There is no

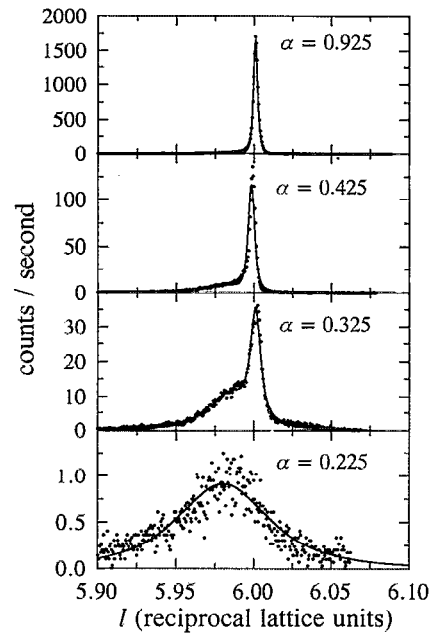


FIG. 2. $[00.1]$ scans through Al_2O_3 (11.6) peak at different angles of incidence α (in degrees). Scans were corrected for refraction and fit with Pearson-7 line shapes.

shift in the position of the peak center, verifying that *on average* the implanted layer remains constrained by the substrate in-plane, despite some local strain at the surface.

Representative $[00.1]$ scans through the (11.6) peak of the 10^{17} sample are shown in Fig. 2. Each plot has been shifted to correct for the index of refraction for pure Al_2O_3 . Above the critical angle ($\alpha = 0.325, 0.425$, and 0.925), each scan is fit by two Pearson-7 peaks.²³ The substrate peak at $l = 6$ is resolution limited and decreases in intensity as the penetration depth decreases. Its low l shoulder varies little in intensity and width above the critical angle. Below the critical angle ($\alpha = 0.225$), the scan is fit by a single peak at the position of the shoulder, which is now broader and less intense because the penetration depth is less than the thickness of the implanted layer. Because it becomes relatively much stronger at a small glancing angle, we identify the shoulder as scattering from the near-surface implanted layer. A scan through the (11.3) peak verifies that the shift of the shoulder relative to the peak is due to a strain of 0.0033 ± 0.0017 . Below the critical angle, low intensity and peak broadening limit accuracy; above the critical angle, accuracy is limited by overlap with the substrate peak and uncertainty in the index of refraction. Note that below the critical angle the peak shift is independent of the index of refraction. Within the above uncertainty, the lattice constant is the same for the near-surface region observed below the critical angle and for the entire implanted region as observed above the critical angle. Data from the 4×10^{16} sample are consistent with the same strain observed for 10^{17} . The width of the shoulder, above the critical angle, corresponds to a particle size of 50 nm, indicating that a large fraction of the ~ 80 nm ion-damaged layer scatters coherently. The difference between the 50 nm particle size and 80 nm implanted layer thickness may be

attributed to dislocations or other extended defects; since the crystalline surface is strained into registry with the substrate, the presence of a buried amorphous layer is unlikely.

To determine the concomitant in-plane stress, we assume that implantation would produce an isotropic expansion D . As observed, the constraint of the substrate prevents in-plane expansion: $\epsilon_{xx}=\epsilon_{yy}=-D$, $\epsilon_{xy}=0$. The crystals are sufficiently thick that we may neglect bending and take $\epsilon_{xz}=\epsilon_{yz}=0$. The only stress is

$$\sigma_{xx}=\sigma_{yy}=c_{13}\epsilon_{zz}-(c_{11}+c_{12})D. \quad (2)$$

Because the film is unconstrained normal to the substrate, we have

$$\sigma_{zz}=c_{33}\epsilon_{zz}-2c_{13}D=0. \quad (3)$$

From Eqs. (2) and (3), the elastic constants for Al_2O_3 ,²⁴ and the observed $D+\epsilon_{zz}=0.0033$, we have $D=0.0023$ and $\sigma_{xx}=1.4\pm 0.7$ GPa. These stresses are in good agreement with average stresses inferred from the indentation measurements of integrated stress in Cr^+ -implanted Al_2O_3 ,⁶ but an order of magnitude less than those inferred from bending measurements of samples implanted with Ti^+ with similar total damage energy.⁸ These results verify that the measurement of indentation crack length gives reasonable values for residual stress and can serve as a rapid test of surface treatment.

If we assume that cracks must initiate at the surface, the 1.4 GPa we observe will simply increase the yield strength by 1.4 GPa. The observed increase in the yield strength of Cr^+ -implanted sapphire is between 0.37 and 0.54 GPa.⁶ To understand this relatively small increase, we compare the depth of implantation to the depth of the flaws which lead to rupture. As pointed out by Griffith,²⁵ a necessary condition for crack propagation is that the fracture energy required to extend the crack be less than the energy gained by stress relief, which requires that $\sigma_{xx} < (2ET/\pi\nu C)^{1/2}$, where σ_{xx} is the yield stress, $E=400$ GPa is Young's modulus, $T=6$ J/m² is the fracture toughness, $\nu=0.235$ is Poisson's ratio, and C is the crack length.²⁶ The median rupture stress for unimplanted samples is 0.79 GPa, implying a crack depth C of at least 10 μm . Ion implantation to a depth of 80 nm is of limited effectiveness in reducing the stress at the tip of a crack this deep.

In conclusion, we have applied glancing incidence x-ray diffraction techniques to determine the surface stress in ion-implanted sapphire crystals. We measure a compressive stress of 1.4 ± 0.7 GPa, consistent with indentation measurements. We find that the surface stress to be independent of dose over the range of 4×10^{16} – 1×10^{17}

ions/cm². This is twice the stress obtainable by more traditional processing such as thermal quenching and chemical treatment,²⁷ and accounts for the large increase in flexure strength. The Griffith criterion for crack propagation suggest that implantation to a depth of several microns is required to realize the greatest yield strength.

We are grateful to M. O'Hern, L. Romana, and J. E. Pawel for assistance in sample preparation and to F. J. Walker for helpful discussions. This work was sponsored by the Division of Materials Sciences, U.S. Department of Energy, under Contract No. DE-AC05-84OR21400 with Martin Marietta Energy Systems, Inc.

¹R. L. Barnett and P. C. Hermann, in *Fracture*, edited by H. Liebowitz (Academic, New York, 1969), Vol. IV, pp. 173–274.

²H. P. Kirchner, *Strengthening of Ceramics* (Dekker, New York, 1979).

³C. W. White, C. J. McHargue, P. S. Sklad, L. A. Boatner, and G. C. Farlow, *Mater. Sci. Rep.* **4**, 41 (1989).

⁴T. Hioki, A. Itoh, S. Noda, H. Doi, J. Kawamoto, and O. Kamigaito, *Nucl. Instrum. Methods B* **7/8**, 521 (1985).

⁵T. Hioki, A. Itoh, M. Ohkubo, S. Noda, H. Doi, J. Kawamoto, and O. Kamigaito, *J. Mater. Sci.* **21**, 1321 (1986).

⁶C. J. McHargue, M. E. O'Hern, C. W. White, and M. B. Lewis, *Mater. Sci. Eng. A* **115**, 361 (1989).

⁷C. J. McHargue, in *Structure-Property Relationships in Surface-Modified Ceramics*, edited by C. J. McHargue (Kluwer Academic, Norwell, MA, 1989), pp. 253–273.

⁸P. J. Burnett and T. F. Page, *J. Mater. Sci.* **20**, 4624 (1985).

⁹E. N. Bunting, *J. Res. Natl. Bur. Stand.* **6**, 947 (1931).

¹⁰K. Komenou, I. Hirai, K. Asama, and M. Sakai, *J. Appl. Phys.* **49**, 5816 (1978).

¹¹V. S. Speriosu, H. L. Glass, and T. Kobayashi, *Appl. Phys. Lett.* **34**, 539 (1979).

¹²B. C. Larson and J. F. Barhorst, *J. Appl. Phys.* **51**, 3181 (1980).

¹³R. Kaufmann, G. Linker, and O. Meyer, *Nucl. Instrum. Methods* **191**, 532 (1981).

¹⁴B. E. MacNeal and V. S. Speriosu, *J. Appl. Phys.* **52**, 3935 (1981).

¹⁵V. S. Speriosu, B. M. Paine, M.-A. Nicolet, and H. L. Glass, *Appl. Phys. Lett.* **40**, 604 (1982).

¹⁶C. R. Wie, *Nucl. Instrum. Methods B* **9**, 25 (1985).

¹⁷C. R. Wie, T. A. Tombrello, and T. Vreeland, Jr., *J. Appl. Phys.* **59**, 3743 (1986).

¹⁸S. I. Rao, C. R. Houska, K. Grabowski, J. Clauassen, G. Ice, and A. Habenschuss, in *Characterization of the Structure and Chemistry of Defects in Materials*, edited by B. C. Larson, M. Ruhle, and D. N. Seidman (Materials Research Society, Pittsburgh, PA, 1989), MRS Symposium Proceedings Vol. 138, pp. 87–92.

¹⁹G. Wallner, E. Burkel, H. Metzger, J. Peisl, and S. Rugel, in *Synchrotron Radiation in Materials Research*, edited by R. Clarke, J. Gland, and J. H. Weaver (Materials Research Society, Pittsburgh, PA, 1989), MRS Symposium Proceedings Vol. 143, pp. 19–24.

²⁰I. Manning and G. P. Mueller, *Nucl. Eng. Design* **33**, 78 (1975).

²¹S. G. J. Mochrie, *J. Appl. Cryst.* **21**, 1 (1988).

²²G. H. Vineyard, *Phys. Rev. B* **26**, 4146 (1982).

²³M. M. Hall, Jr., V. G. Veeraraghavan, H. Rubin, and P. G. Winchell, *J. Appl. Cryst.* **10**, 66 (1977).

²⁴J. H. Gieske and G. R. Barsch, *Phys. Status Solidi* **29**, 121 (1968).

²⁵A. A. Griffith, *Philos. Trans. R. Soc. London Ser. A* **221**, 163 (1921).

²⁶E. Dörre and H. Hübner, *Alumina* (Springer, Berlin, 1984), pp. 76, 82.

²⁷E. Dörre and H. Hübner, *Alumina* (Springer, Berlin, 1984), pp. 184–187.